Role of Computed Tomography and Magnetic Resonance Imaging in the Diagnosis of Coronary Artery Disease: Indications and Applications

Mona Bhatia[1] Parveen Kumar[1]

[1] Department of Radiodiagnosis and Imaging, Fortis Escort Heart Institute, New Delhi, India

Indographics 2022;1:41–56.

Address for correspondence Mona Bhatia, MD, FRCR(UK), FSCCT (USA), FSCMR(USA), Department of Radiodiagnosis and Imaging, Fortis Escort Heart Institute, New Delhi 110025, India (e-mail: monabhatia1@gmail.com).

Abstract

Coronary artery disease (CAD) is the leading cause of death worldwide. The diagnosis of CAD relies on the clinical history, electrocardiographic changes, and imaging findings. The available imaging methods include transthoracic echocardiography, computed tomography (CT), cardiac magnetic resonance (CMR) imaging, and invasive angiography. Over the last two decades, cardiac CT and CMR have emerged as promising noninvasive modalities in the assessment of patients with suspected and established CAD. Both the modalities have their own advantages and disadvantages which complement each other in comprehensive evaluation of CAD aiding in the diagnosis, guiding clinical decision-making, and improving risk stratification. In this article, we provide an overview of the techniques and clinical applications of cardiac CT and CMR imaging in the assessment of patients with CAD.

Keywords

- coronary artery disease
- computed tomography
- magnetic resonance imaging

Introduction

Coronary artery disease (CAD) remains the most common cause of morbidity and mortality in developed countries.[1] There has been an explosive growth in the cardiovascular imaging technology in last decade presenting new opportunities to the physicians to gain important information about the patient's condition. Among the armamentarium of the noninvasive diagnostic tools, cardiac computed tomography (CT), and cardiovascular magnetic resonance (CMR) imaging have emerged as robust diagnostic tools guiding the clinical decision-making. The scope of cardiac CT has widened from calcium scoring and coronary computed tomographic angiography (CCTA) to include newer applications, such as myocardial perfusion imaging, dual-energy CT, and CT-derived fractional flow reserve enabling integrated assessment of cardiac morphology, function, perfusion, and viability.[2,3] CMR is a multiparametric, multiplanar imaging technique which allows an accurate determination of biventricular function and precise evaluation of myocardial structure, perfusion, and tissue characteristics in a single study of 35 to 40 minutes.[4] The review presented here focuses on role of cardiac CT and CMR in the evaluation of CAD. The first part describes the clinical value and potential applications of cardiac CT in detecting CAD, myocardial viability, and perfusion. In the second part, the range of applications of CMR is discussed in coronary artery imaging, acute coronary syndrome, and chronic ischemic heart disease.

DOI https://doi.org/10.1055/s-0042-1742571.

Thieme Medical and Scientific Publishers Pvt. Ltd., A-12, 2nd Floor, Sector 2, Noida-201301 UP, India

Role of Cardiac Computed Tomography in Coronary Artery Disease

The clinical utility of cardiac CT is rapidly improving due to technical innovations addressing the current limitations of the modality. This is especially true in context to CCTA which has emerged as robust and widely embraced tool in clinical practice guiding patient management.[4] The emerging newer applications like dual-energy CT, CT myocardial perfusion, and CT-derived FFR have enhanced the domain of cardiac CT by providing conclusive information about all aspects of CAD including myocardial perfusion and viability.[2,5] The evidence-based data on the outcomes, prognosis, and cost-effectiveness of cardiac CT are increasing exponentially. A brief review about the clinical applications and their current role in clinical practice is discussed below.

Coronary Artery Calcium Score

Calcification of coronary arteries occurs by means of an active process of mineralization with deposition of hydroxyapatite crystals. It begins in the early stages of atherosclerosis. Since atherosclerosis is the major culprit factor for the development of clinical CAD, it is important to identify high-risk individuals harboring advanced atherosclerosis in early stages. There is large body of evidence that coronary artery calcium (CAC) determined with CT is an equivalent measure for coronary atherosclerotic burden in adults. Study has shown a direct relationship between CAC measured at CT and histologically measured atherosclerotic plaque burden. The first formal CT based CAC score was introduced in 1990, followed by many different CAC scores with varying strengths, weaknesses, and limitations. The traditional scoring methods include Agatston's score, volume score, mass score, calcium coverage score, and visual score.[6] Agatston's score (AS) is the most widely used CAC score in clinical practice. The score has been adapted to multi-detector computed tomography (MDCT) using 120 KVp, and variable mA according to the body weight with 3-mm slice thickness. It considers the lesions with CT attenuation value >130 HU and area ≥ 1 mm^2. The individual lesion score is calculated by multiplying the lesion area with density weighting factor. The individual scores are then added irrespective of the distribution and location to determine the total Agatston score.[7] The research in the last decade has identified several strategies to standardize the reporting of CAC to facilitate clinical communications and implement appropriate patient management. A new standardized reporting system, CAC–data and reporting system (DRS), has been introduced recently in 2018 by the Society of Cardiovascular Computed Tomography (SCCT).

The purpose of CAC–DRS classification is to standardize the reporting of coronary artery calcium. It is applicable on both gated and nongated chest CT scans. It recommends using Agatston's or visual score. There are four categories in this classification ranging from CAC–DRS of 0 to CAC–DRS of 3. In case the Agatston method is used, the total Agatston score is assigned into one of the four CAC–DRS risk categories, including CAC–DRS 0 = Agatston's score 0, CAC–DRS 1 = Agatston's score 1–99, CAC–DRS 2 = Agatston's score 100–299, and CAC–DRS 3 = Agatston's score >300. Similarly, with the visual method, the none, mild, moderate, and severe grades correspond to CAC–DRS 0, 1, 2, and 3 categories, respectively. There are two modifiers in the CAC–DRS classification. The first modifier denotes the type of scoring system: Agatston's or visual estimation represented by A and V letters, respectively. The second modifier represents the number of vessels involved and is represented by letter N. It varies from N1 to N4 depending on the number of coronary arteries involved, namely, left main (LM), left circumflex (LCx), left anterior descending (LAD), and right coronary artery (RCA). Two multipliers are separated by symbol "/" slash[8] (►**Fig. 1**).

CAC–DRS has been validated in multiple studies. Large retrospective studies conducted by Dzaye et al have shown a direct correlation between all-cause mortality rate and CAC–DRS score.[9] Another large retrospective study done by Osawa et al has shown that CAC-DRS is independently associated with the incidence of major adverse cardiac events (MACEs) and MACEs or all-cause death.[10]

Computed Tomography Coronary Angiography

The catheter angiography is the gold-standard technique for the evaluation of CAD. However, the risk of serious complications associated with catheter angiography, together with economic deliberations and inconvenience to the patient, has prompted for the search of a noninvasive modality. CT coronary angiography has emerged as the most promising alternative to catheter angiography for assessing coronary arteries. The diagnostic performance of CCTA has been validated by large number of studies. CCTA has shown a high sensitivity and high negative predictive value (NPV) for detecting morphologically significant CAD, compared with catheter angiography. The reported sensitivity of CCTA for detecting hemodynamically significant CAD is 95% or higher, and the NPV is as high as 99 to 100%.[11–13] These results have significantly encouraged the use of CCTA in daily clinical practice worldwide. The implementations of the guidelines and recommendations of various national and international societies have further enhanced its role in diagnosing and excluding CAD.[14–16] The most common indication for CCTA is the evaluation of chest pain with intermediate pretest probability of CAD and uninterpretable electrocardiography (ECG), or if the patient is unable to do exercise. Patients with high pretest probability are ideal candidates for catheter angiography. The role of CCTA in patients with low pretest probability is uncertain.[17]

The interpretation of CCTA images can be done visually or by using digital tools. The quantification of luminal stenosis (area and diameter) assists in interpretation and conveys a quantitative information to the clinician. Studies have demonstrated a good correlation between CCTA-derived maximum diameter stenosis and invasive angiography or intravenous ultrasound but with a large standard deviation.

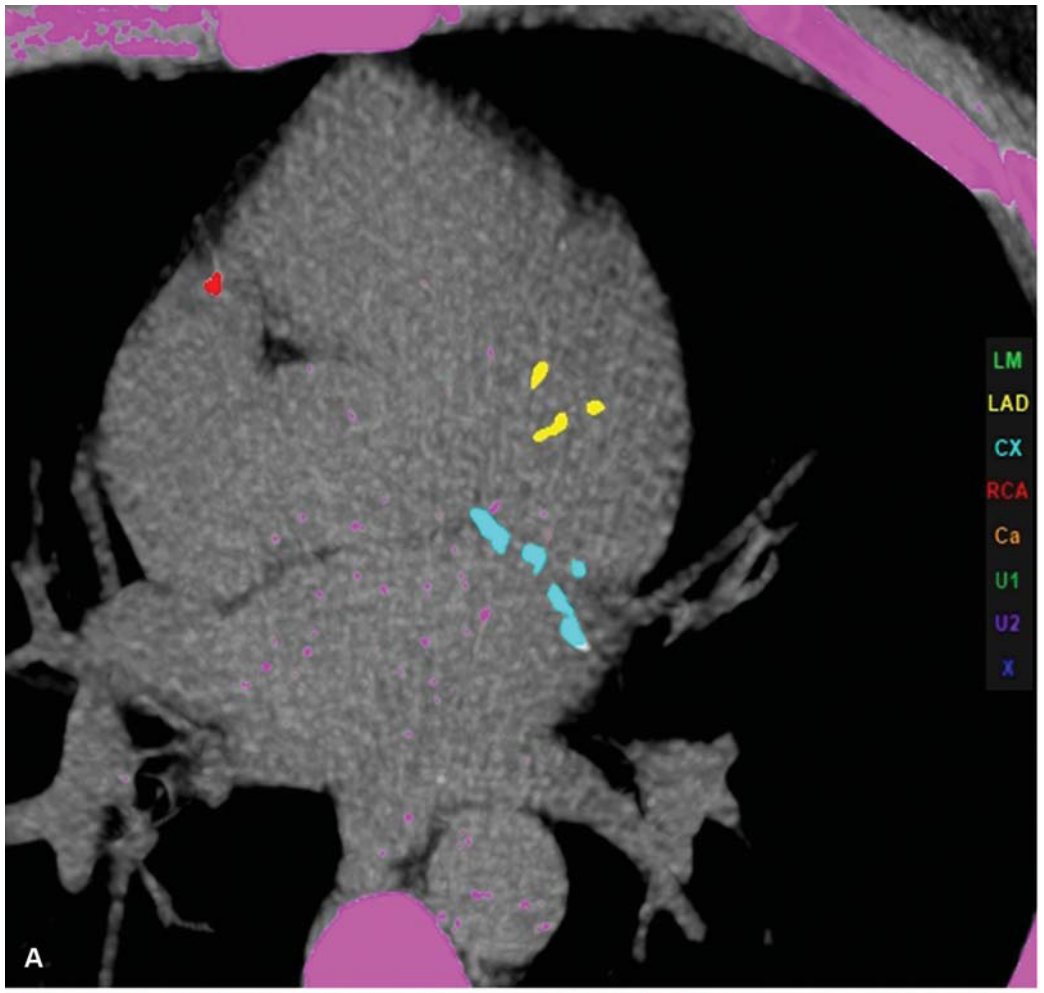

Artery	Lesions	Volume / mm³	Equiv. Mass / mg	Score
LM	0	0.0	0.00	0.0
LAD	3	53.4	10.05	52.9
CX	5	370.6	91.32	447.1
RCA	1	28.9	5.43	34.6
Ca	0	0.0	0.00	0.0
Total	**9**	**452.8**	**106.80**	**534.6**
U1	0	0.0	0.00	0.0
U2	0	0.0	0.00	0.0

Settings
Score Type: Agatston equivalent, Threshold: 130 HU (105.3 mg/cm³ CaHA)
Mass calibration factor: 0.81
B

Fig. 1 (**A, B**) CAC-DRS A3/N3 and V3/N3. CAC is severe (534.6) on Agatston (A3) and visual (V3) analyses. Three vessels are involved (N3). Calcium in LAD, RCA and LCx are represented by yellow, red and sky-blue color respectively. CAC, coronary artery calcium; DRS, data and reporting system; LAD, Left anterior descending artery; LCx, Left circumflex artery; LM, left main artery; RCA, Right coronary artery.

The comparative studies suggest that CCTA derived values correlates with invasive angiography to within 25% at the best.[18–21] The commonly recommended stenosis grading scale is as follows.

- 0, normal: absence of plaque and no luminal stenosis.
- 1, minimal: plaque with <25% stenosis.
- 2, mild: 25 to 49% stenosis.
- 3, moderate: 50 to 69% stenosis.
- 4, severe: 70 to 99% stenosis.
- 5: occluded.

Multiple societies in the cardiology and radiology have introduced the CAD–Reporting and Data System (CAD–RADS) as a collaborative effort. The purpose of CAD–RADS is to provide a standard classification of CAD integrated with patient-specific clinical care. There are six CAD–RADS categories ranging from CAD–RADS 0 (no plaque) to CAD–RADS 5 (at least one total occlusion). CAD-– 4 is further divided into 4A and 4B. The category is assigned on the basis of highest grade of stenosis. CAD–RADS 0 corresponds to no atherosclerotic disease in any coronary artery; CAD-RADS 1 corresponds to a single maximum stenosis of 1 to 24%; CAD–RADS 2 corresponds to a single maximum stenosis of 25 to 49%; CAD–RADS 3 corresponds to a single maximum stenosis of 50 to 69%; CAD–RADS 4A corresponds to single or two vessel stenosis of 70 to 99%; CAD–RADS 4B corresponds to three vessel stenosis of 70 to 99% or a single 50 to 99% stenosis in left main artery (LM); and CAD–RADS 5 represents total occlusion of at least one vessel. CAD–RADS also provides the information about image quality (N), stents (S), plaque characteristics (V), and coronary artery bypass grafts (G; ►**Figs. 2–4**). The final CAD-RADS category provides an interpretation of the imaging findings together with recommendations for further cardiac workup and management.[22]

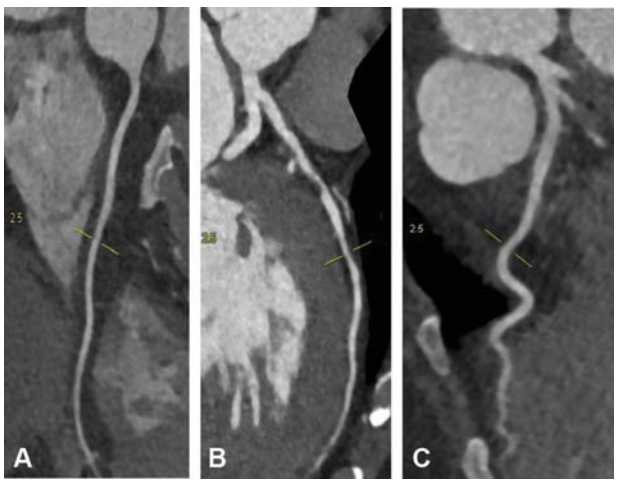

Fig. 2 CAD-RADS 3. (**A**) Coronary CT angiography curved multiplanar reconstruction of the RCA shows normal caliber without any atherosclerotic disease. (**B**) Proximal LAD shows moderate stenosis (60–70%) in proximal part (red arrow) due to mixed plaque. (**C**) LCx is normal. CAD, coronary artery disease; CT, computed tomography; LAD, left anterior descending artery; LCx, left circumflex artery; RADS, reporting and data system; RCA, right coronary artery.

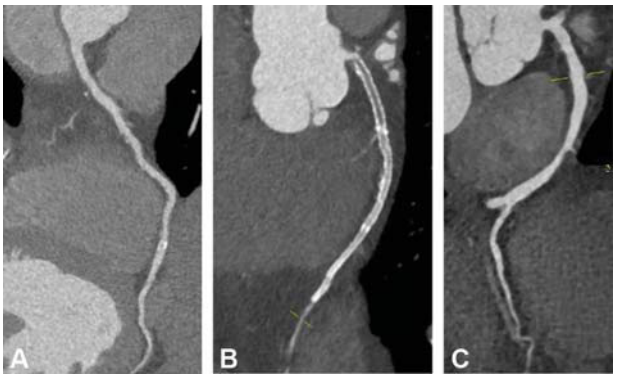

Fig. 3 CAD-RADS 5/S. (**A**) Coronary CT angiography curved MPR image of RCA shows multiple calcified and noncalcified plaques causing minimal stenosis. (**B**) Coronary CT angiography curved MPR image of LAD shows a stent in proximal part with total luminal occlusion. (**C**) Coronary CT angiography curved MPR image of LCx shows normal course and caliber. CAD, coronary artery disease; CT, computed tomography; LAD, left anterior descending artery; LCx, left circumflex artery; MPR, multiplanar reconstruction; RCA, right coronary artery.

Fig. 4 CAD-RADS 5/G. (**A**) LIMA-LAD graft shows good opacification with normal proximal and distal anastomotic sites. (**B**) SVG-distal RCA graft shows wall calcification and total thrombotic occlusion. LCx was nondominant and normal (not shown). LAD, left anterior descending artery; LCx; left circumflex artery; RCA, right coronary artery; SVG; saphenous vein graft.

CCTA is helpful in the evaluation of stents. Coronary stents are broadly classified into two categories; metallic and bioabsorbable (BVS). The improved hardware configuration of latest generation CT scanners allows direct visualization of the metallic stent struts, while nonmetallic BVS are identified by the dot-like platinum markers at proximal and distal ends (►**Fig. 5**). The common stent-related complications include in-stent restenosis (ISR), thrombosis and stent fracture. Earlier studies using 16- and 64-slice MDCT have shown a greater difference in the sensitivity for detecting ISR, 54% in stents with a diameter of ≤3 mm to 86% in stents >3 mm.[23] However, the recent third-generation dual-source CT enables accurate diagnosis of ISR in all size stents with preserved image quality and low radiation dose.[24] There are few challenges in the CT imaging of coronary stents. These include blooming artifacts, geometric effects due to cardiac anatomy, motion artifacts, and intravascular contrast

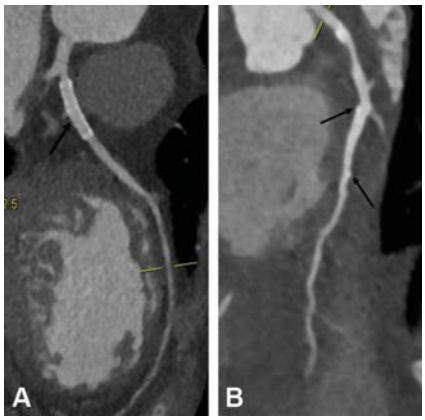

Fig. 5 Types of stents. (**A**) Coronary CT angiography curved multiplanar reconstruction of the LAD shows a patent metallic stent in proximal part identified by metallic struts (black arrow). (**B**) Coronary CT angiography curved multiplanar reconstruction of the LAD shows a BVS stent in mid part identified by two radiopaque platinum markers proximally and distally (black arrows). BVS, bioabsorbable; CT, computed tomography; LAD, left anterior descending artery.

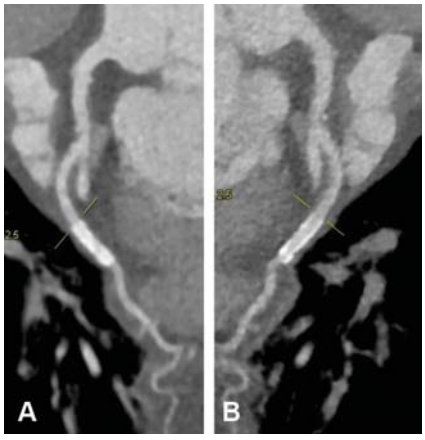

Fig. 6 Visibility of coronary stent lumen with different convolution filters. The most appropriate filter should be chosen to achieve balance between the visibility of low-contrast structures and the quantity of image noise. (**A**) Coronary CT angiography curved multiplanar image of LCx reconstructed with a smooth convolution filter (B38f) shows barely visible stent lumen. (**B**) The image reconstructed with a dedicated edge-enhancing kernel (B45f) allows good visualization of stent lumen. CT, computed tomography; LCx; left circumflex artery.

enhancement. Blooming describes an effect where the stent struts appear to be thicker, leading to underestimation of the stent lumen. It is more pronounced in bifurcation lesions (Y, V, or T techniques) and in the presence of overlapping stent placements. The commonly used technique to decrease blooming artifacts are high kV imaging and sharp convolution kernels (►**Fig. 6**). Motion artifacts due to breathing or cardiac motion pose another problem making study nondiagnostic. It causes blurring and disproportionally exacerbates the blooming artifacts. Decreasing the heart rate and increasing the temporal resolution are the standard approaches toward this issue. It has been seen in several phantom studies that the angulation of stent from the scan plan has a potential effect on the visibility of stent lumen. The lumen is best visible if the stent is located at 0 or 90 to the z-axis. The course of coronary arteries is typically angulated except for the midpart of RCA. This angulated anatomy also added to the difficulties in the stent evaluation. A sufficient contrast enhancement is the prerequisite for CCTA. This is of even more importance in stents evaluation as sharp convolution filters and beam hardening negatively affect contrast-to-noise ratio. Increasing the rate of contrast administration and appropriate voltage selection allows good intravascular attenuation to permit delineation of neointima hyperplasia or ISR inside the stent.[25]

CTA is an accurate method for assessing coronary artery bypass grafts (CABG) patency also. The commonly used grafts are internal mammary artery, radial artery, and saphenous venous grafts. The graft is usually divided into following three different segments: (1) the proximal anastomosis, (2) the body of the graft, and (3) the single (or sequential) distal anastomosis. The graft patency is assessed for regular shape and border of graft wall with homogeneous, contrast-enhancement of the graft lumen. The common graft-related complications include graft stenosis, occlusion, spasm, and aneurysm. There is extensive evidence that CCTA is highly accurate in the evaluation of CABG. In the meta-analysis study, Barbero et al reviewed 959 patients' CABG operations with 1,586 arterial and venous grafts. These patents were evaluated using 64-slice MDCT scanners of different vendors. Both the sensitivity and specificity of CCTA in detecting complete graft occlusions were 99% in comparison to invasive coronary angiography.[26]

Another important advantage of CCTA is plaque imaging. Although, intravenous ultrasound (IVUS) is the imaging reference for characterizing coronary artery plaques, but it is an invasive technique and not justifiable in asymptomatic patients. CCTA, beyond its ability to quantify luminal stenosis is helpful in detection and characterization of coronary atherosclerotic plaques.[27] The plaques are classified into calcified, mixed, and noncalcified types. The qualitative and quantitative assessment of plaques is targeted at plaque size, plaque composition, and plaque remodeling. The plaques of potential clinical importance tend to be larger in size, often located in proximal coronary arterial segments, and have a sizeable necrotic core. The so called vulnerable or high-risk plaque refers to the atherosclerotic lesions with features associated with future acute coronary events. There are four main features of vulnerable plaque on CCTA as follows: (1) positive remodeling defined as outer vessel diameter at the plaque $\geq$1.1 times that of adjacent uninvolved vessel; (2) low attenuation defined as $<$30 HU; (3) napkin-ring sign defined as peripheral higher attenuation of the noncalcified portion of the plaque; and (4) spotty calcium defined as calcific foci $<$3 mm in any direction (►**Fig. 7**). The prognostic value of the suspected CT features of the vulnerable plaque have been validated in multiple retrospective and prospective studies. The first prospective observational study by Motoyama et al has reported that both positive remodeling and low attenuation plaque are independent predictors for the occurrence of MACE in short-term

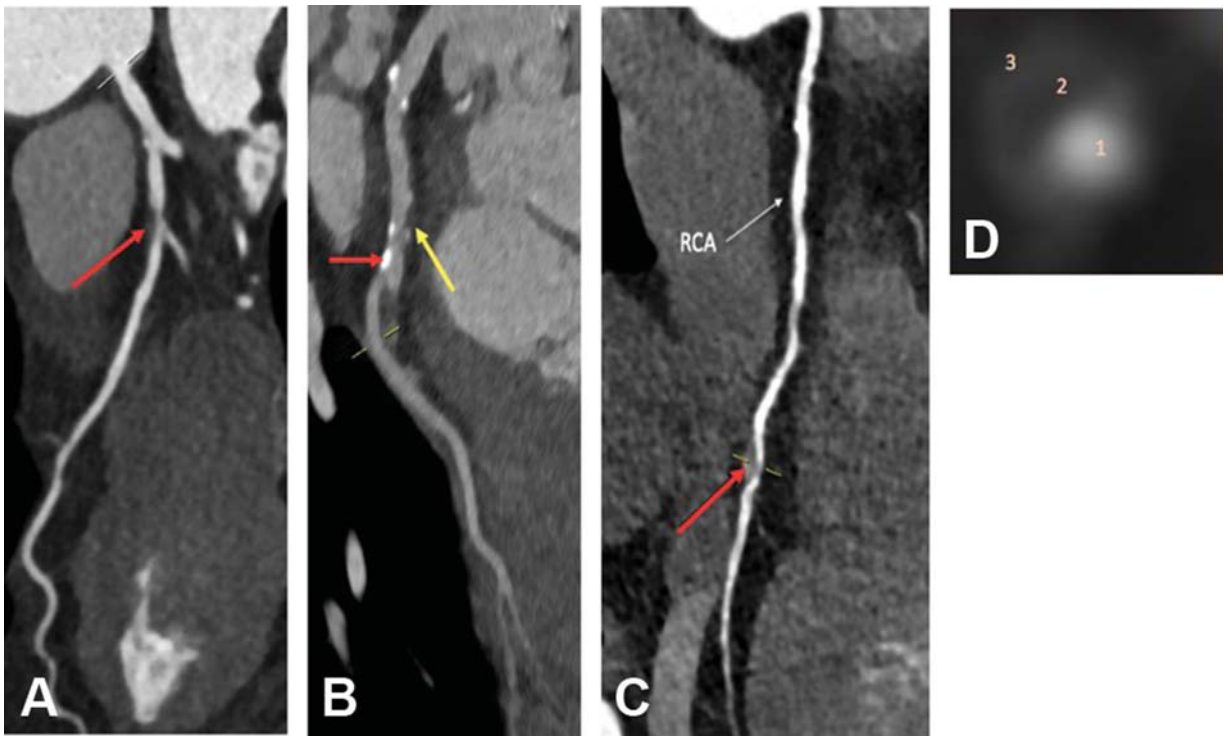

Fig. 7 Types of plaques. (**A**) Coronary CT angiography curved MPR image of LAD shows a noncalcified plaque in proximal part. (**B**) Coronary CT angiography curved MPR image of LCx shows calcified (red arrow) and mixed plaques (yellow arrow). (**C**) Curved MPR CT angiographic image and (**D**) corresponding axial reformatted image of RCA shows a vulnerable plaque with napkin-ring sign. Axial reformatted CT angiographic image perpendicular to the vessel lumen (1, CT number = 380 HU) shows central low-attenuation core (2, CT number = 25 HU) and outer circumferential high-attenuation area (3, CT number = 98 HU) representing napkin-ring sign. CT, computed tomography; LAD, left anterior descending artery; LCx; left circumflex artery; RCA, right coronary artery.

follow-up, whereas spotty calcification was not.[28] Another prospective study with 895 patients and a mean follow-up of 2.3 years has shown that the napkin-ring sign in addition to low attenuation plaque and positive remodeling is independently associated with a composite end point of acute coronary syndrome and cardiac death.[29] The Rule Out Myocardial Ischemia/Infarction Using Computer Assisted Tomography (ROMICAT-II) trial investigated the patients presenting to the emergency with acute chest pain having negative initial troponin and ECG by CCTA imaging. It was concluded that the presence of any of the vulnerable plaque features is an independent predictor for the presence of acute coronary syndrome (ACS).[30] This data suggests that CCTA might have a prognostic role in patients with ACS.

Computed Tomography Viability Imaging and Perfusion

CCTA plays an important role in anatomical and morphological assessment of coronary artery plaques and stenosis but it does not provide information about the hemodynamic significance of the lesion. The commonly available diagnostic modalities for functional imaging include stress echocardiography, single–photon emission CT (SPECT), positron emission tomography (PET), and magnetic resonance imaging (MRI). CT myocardial perfusion is a newer technique that provides functional assessment of the myocardium and is commonly referred as "one-stop-shop" for a comprehensive assessment of CAD.[31]

There are two approaches for performing CT myocardial perfusion,[1] static arterial first-pass imaging and[2] dynamic time-resolved imaging. Static arterial first-pass imaging provides a single-phase snapshot of myocardial attenuation during early arterial phase. It can be done using single-energy or dual-energy CT (DECT). Dynamic CT myocardial perfusion imaging uses serial acquisitions of the myocardium throughout the cardiac cycle to track the kinetics of contrast media distribution during the initial pass, arterial phase, and microcirculation, and provides absolute quantitative measurements of myocardial blood flow and volume.[32] The protocol of CT myocardial imaging includes stress and rest acquisitions similar to cardiac MRI and nuclear imaging. It is essential to perform the scan during the early portion of first-pass circulation, as there occurs rapid wash-out of contrast agent due to diffusion into extravascular space. The contrast injection rate should be kept higher, at least 5 mL/s, for optimizing the strength of enhancement in the first-pass arterial phase. There are two different protocols named according to sequence of scan acquisitions, rest/stress or stress/rest. The commonly used pharmacological stress agents are adenosine, regadenoson, dipyridamole, and dobutamine. An interval of 10 to

15 minutes between the two sequences is necessary for the optimal contrast wash-out. The best approach is chosen depending on the type of patients' risk. The rest first protocol is reserved for the patients with low-to-intermediate pertest probability of CAD, while stress first is chosen for patients having high pretest probability of lesions associated with ischemia.[33] The different types of CT myocardial perfusion techniques are summarized below.

Static Single Energy Computed Tomography Myocardial Perfusion

The static CT myocardial perfusion imaging is based on acquisition of one single phase during the first-pass of contrast. The challenges involving the maximum contrast enhancement and optimal contrast delivery must be met. The assessment is done using visual qualitative method. Perfusion defects appear as hypodense regions in subendocardial or transmural distribution (►**Figs. 8** and **9**). Thick multiplanar reconstructions (5–8-mm slice thickness) are recommended for assessing perfusion defects due to improved contrast-to-noise ratio. An integrated review of stress and rest images allows differentiation between ischemic and nonischemic myocardium, and if ischemia is present, the combined assessment can mark off viable and nonviable myocardium by characterizing fixed and inducible perfusion abnormalities. Hypoperfusion in stress with normal perfusion in rest indicates ischemia; hypoperfusion in stress persisting with same extent in rest indicates necrosis; hypoperfusion in stress that persists with lesser extension in rest indicates peri-infarct ischemia.[34] Multiple studies have established the clinical feasibility and accuracy of single-energy static myocardial perfusion imaging. Nasis et al conducted a study to determine the diagnostic accuracy of combined 320-detector row CCTA and adenosine stress CT myocardial perfusion imaging in detecting perfusion abnormalities caused by obstructive CAD. Invasive angiography and SPECT myocardial perfusion were used as reference standard. The sensitivity, specificity, positive predictive value (PPV), and NPV of combined CCTA and CT myocardial perfusion was 94, 98, 94, and 98%, respectively.[35] George et al compared the diagnostic performance of CT myocardial perfusion imaging and SPECT perfusion imaging in the diagnosis of anatomically significant CAD. The sensitivity of CT perfusion imaging was higher than that of SPECT, with

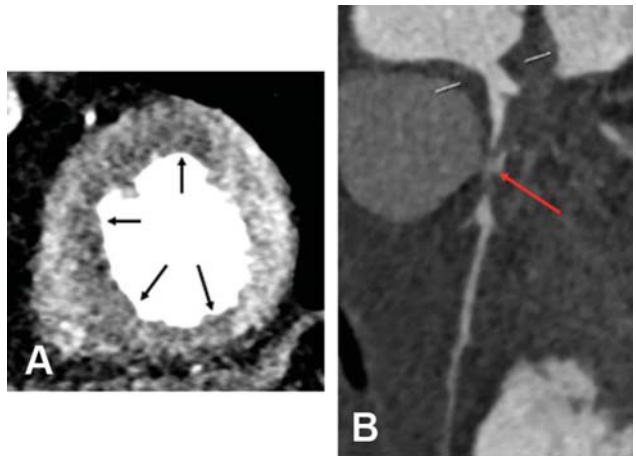

Fig. 9 Static short-axis single energy myocardial perfusion imaging. (**A**) Short-axis and multiplanar images show transmural hypoattenuating perfusion defects (black arrows) in apical anterior, septal and inferior segments. (**B**) Curved multiplanar image of LAD shows total occlusion in the proximal part (red arrow). ; LAD, left anterior descending artery.

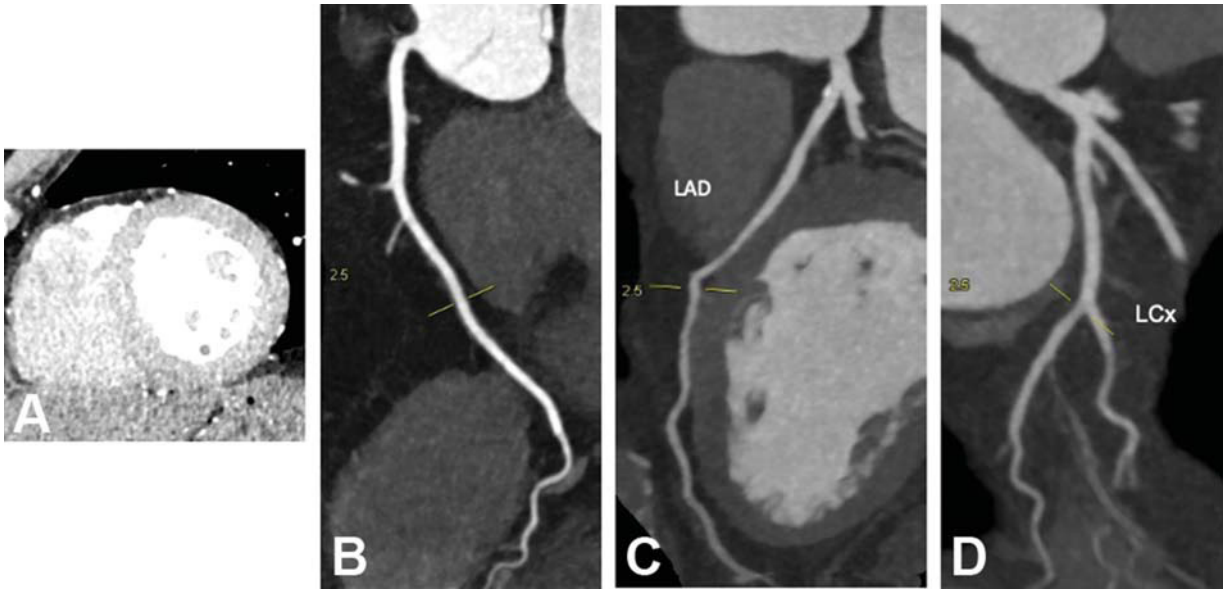

Fig. 8 Static single energy myocardial perfusion imaging. (**A**) Short-axis multiplanar images show no hypoattenuating areas suggestive of perfusion defects in myocardium. (**B–D**) Coronary CT angiography curved multiplanar reconstruction of the RCA, LAD and LCx show normal course and caliber. CT, computed tomography; LAD, left anterior descending artery; LCx; left circumflex artery; RCA, right coronary artery.

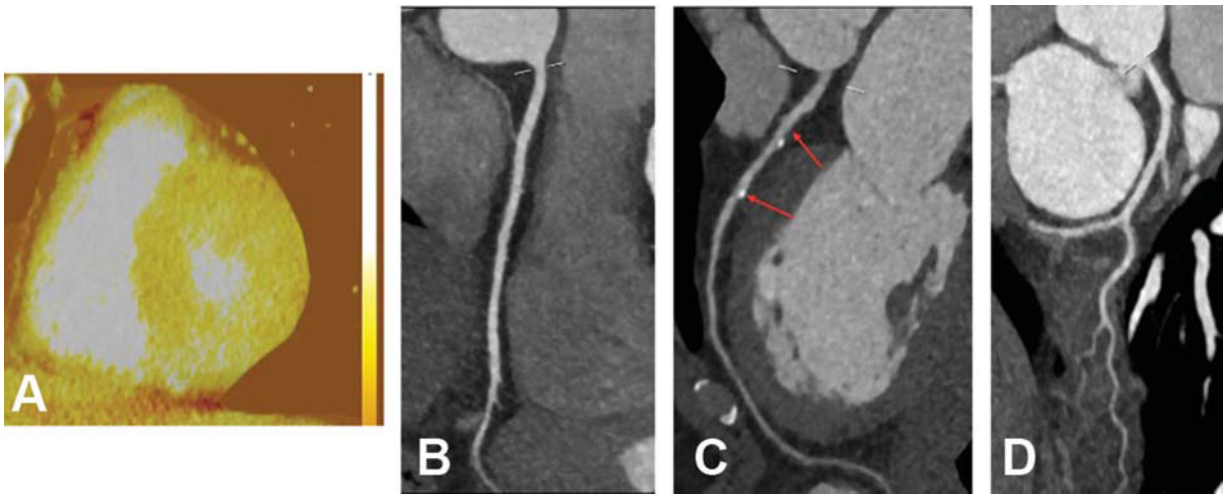

Fig. 10 Static retrospectively ECG gated dual-energy myocardial perfusion imaging. (**A**) Myocardial short axis color-coded iodine distribution map shows no perfusion defects. (**B**) Coronary CT angiography curved multiplanar reconstruction of the RCA shows normal caliber without any atherosclerotic disease. (**C**) LAD shows diffuse mixed disease in proximal and mid part causing minimal luminal stenosis. (**D**) LCx shows normal caliber without any atherosclerotic disease. CT, computed tomography; ECG, electroencephalography; LAD, left anterior descending artery; LCx; left circumflex artery; RCA, right coronary artery.

sensitivities for left main, three-, two-, and one-vessel diseases of 92, 92, 89, and 83%, respectively, for CT perfusion imaging, and 75, 79, 68, and 41%, respectively, for SPECT.[36]

Static Dual Energy Computed Tomography Myocardial Perfusion

DECT myocardial perfusion imaging provides additional information about myocardial composition compared with single-energy CT myocardial perfusion and improves the limitations of single energy CT such as blooming artifacts and beam-hardening artifacts. The assessment of dual energy myocardial perfusion images is done in two different ways:[1] (1) monochromatic analysis, and[2] (2) material decomposition analysis.[37] The images obtained during the scan are "mixed images" which are equivalent to standard CT images at intermediate energy. DECT decomposes the acquired datasets and can reconstruct the simulated ("virtual") monochromatic images ranging from 40 to 140 KeV. The images at 140 KeV resembles a noncontrast acquisition and commonly called as "virtual noncontrast image." The semiquantitative analysis of monochromatic images is done similar to single-energy static perfusion. Different studies have postulated various parameters like absolute contrast enhancement, perfusion index (myocardial contrast enhancement relative to left ventricular enhancement), and transmural perfusion ratio to analyze the monochromatic images; however, visual assessment is still commonly used and has superior diagnostic performance. The material decomposition is the main principle of DECT. This technique allows generation of material specific images. In myocardial perfusion, iodine acts as a surrogate of myocardial blood pool. The generation of iodine maps allows calculation of iodine per mm^3 (iodine density) of the myocardium which represents a semiquantitative estimate of myocardial blood flow, allowing differentiation between normal, ischemic, and infarcted myocardium[38] (►**Figs. 10** and **11**). A myocardial segment with low iodine density on stress, and normal density on rest images represents reversible perfusion defect indicating ischemia. A persistent low-iodine density on both stress and rest images represents a fixed perfusion defect indicating necrosis. Studies have shown that the combined analysis of CCTA and DECT myocardial perfusion imaging outperform the purely anatomic test of CCTA alone in detecting morphologically and hemodynamically significant CAD and reduces the number of false positives in high-risk population.[39–41]

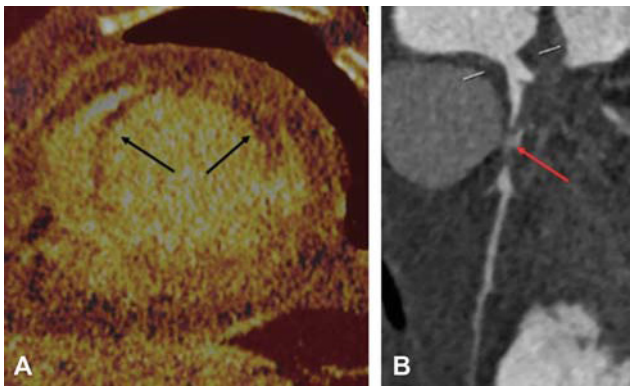

Fig. 11 Static retrospectively ECG gated dual-energy myocardial perfusion imaging. (**A**) Myocardial short axis and color-coded iodine distribution map shows perfusion defects in anterior, anteroseptal and anterolateral segments (black arrows). (**B**) Coronary CT angiography curved multiplanar reconstruction of the LAD shows total occlusion in proximal part (red arrow). CT, computed tomography; ECG, electroencephalography; LAD, left anterior descending artery.

Dynamic Computed Tomography Myocardial Perfusion Imaging

Dynamic CT myocardial perfusion imaging is based on serial acquisitions of the myocardium after contrast administration. The kinetics of contrast media is tracked during the

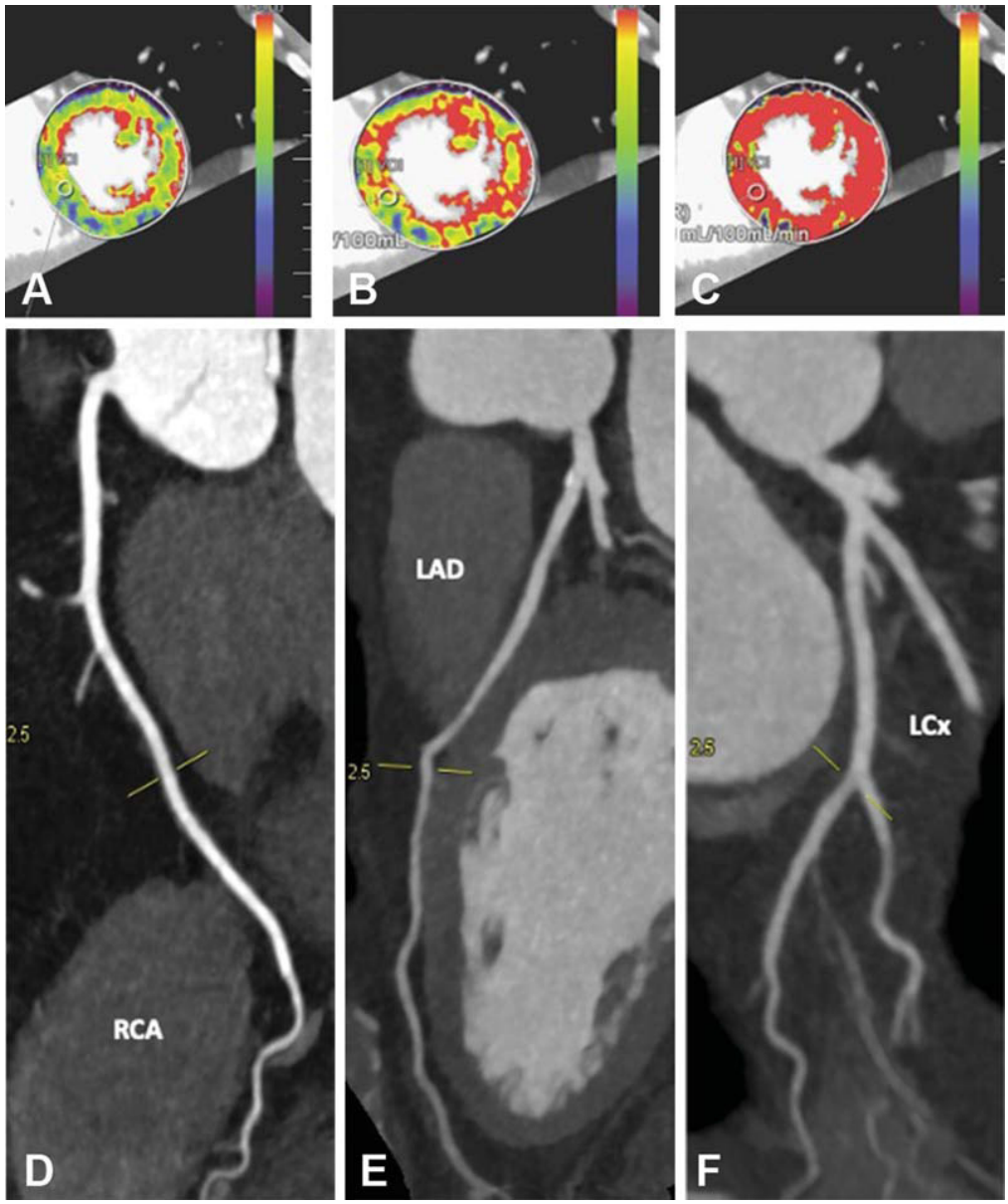

Fig. 12 Dynamic CT perfusion imaging. The color-coded maps of myocardial blood flow (**A**), blood volume (**B**), extraction fraction (**C**) appear normal. The colors of the myocardium are coded according to the flow values with red, green, and yellow representing higher flow values than blue. (**D–F**) Coronary CT angiography curved multiplanar reconstruction of the RCA, LAD and LCx show normal course and caliber. CT, computed tomography; LAD, left anterior descending artery; LCx; left circumflex artery; RCA, right coronary artery.

initial pass, arterial phase, and microcirculation. This has become feasible with the introduction of wide detector CT scanners (256 or 320) which provide full heart coverage with stationary table, or by using shuttle mode in second generation Dual Source scanners in which the table shuttle back and forth between two anatomic positions. The shuttle mode extends the anatomic coverage from 38 to 73 mm. The third-generation DECT scanners provides a larger coverage of 105 mm which allows myocardial perfusion imaging even in dilated hearts as well. End systole (250 ms after the R peak) is the optimal phase for image acquisition. There are two advantages of end systolic phase. First, during systole the myocardial thickness is maximum and apical-to-basal length is shorter which allows whole heart to be scanned. Second, the duration of systole is constant (~200 ms) which decreases the need of contrast and hence the beam-hardening artifacts. The data analysis is done by using semiquantitative and quantitative method. In semiquantitative method, the time attenuation curves are generated which are used to derive various parameters like peak enhancement, time to peak, area under the curve, and attenuation slope. In quantitative method, functional analysis of myocardial blood flow input and output is done and various perfusion parameters like myocardial blood flow (MBF), MBF ratio, and myocardial blood volume (MBV) are derived (►**Figs. 12** and **13**). Various semiautomated softwares are now available which show

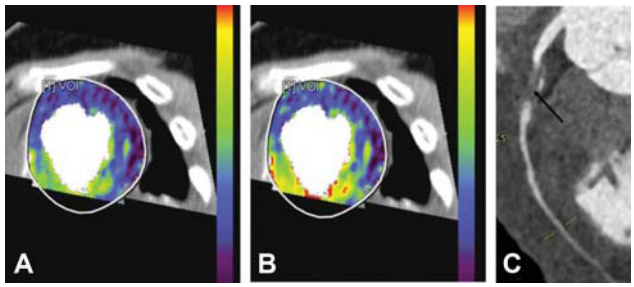

Fig. 13 Dynamic CT perfusion imaging. The color coded maps of myocardial blood flow (**A**), blood volume (**B**), show extensive perfusion defect in anterior, anteroseptal and anterolateral myocardium. The colors of the myocardium are coded according to the flow values with red, green, and yellow representing higher flow values than blue (**C**) Coronary CT angiography curved multiplanar reconstruction of the LAD shows total occlusion of proximal part (arrow). CT, computed tomography; LAD, left anterior descending artery.

similar accuracy to manual analysis.[42] Multiple studies have evaluated the diagnostic performance of dynamic CT myocardial perfusion compared with different non-invasive modalities. Bastarrika et al have compared stress dynamic CT myocardial perfusion with CMR. The sensitivity, specificity, PPV and NPV were found to be 86.1, 98.2, 93.9, and 95.7%, respectively.[43] Ho et al compared dynamic CT-MPI on a 128-slice DECT using dipyridamole to SPECT. The reported sensitivity, specificity, PPV, and NPV were 83, 78, 79, and 82%, respectively.[44]

Computed Tomography Fractional Flow Reserve

Fractional flow reserve (FFR) is a technique to evaluate the hemodynamic significance of CAD. It is defined as the ratio of maximum flow achievable in stenotic artery to the maximum flow achievable if the same artery is normal. It is routinely calculated during invasive catheter (ICA). The technique involves placing a pressure wire across the stenosis, inducing the hyperemia by injecting adenosine and calculating the pressure gradient across the stenosis. This translesional pressure ratio during maximum flow defines the "functional significance" of a coronary lesion.[45] Studies have indicated that a FFR <0.8 can be used as a reliable cut-off for hemodynamic-relevant stenosis.[46]

Recently, CT angiography has developed as a new noninvasive technique for the calculation of FFR. A complex mathematical model incorporating fluid dynamics is used to derived the FFR values across a stenotic lesion.[47] There is high per-patient and per-vessel agreement between CT derived FFR values and invasive FFR using the threshold of 0.80 for both techniques. A poststenotic CT-FFR value less than or equal to 0.80 indicates the possibility of hemodynamic significance while a value greater than 0.80 indicates that the lesion is unlikely to be hemodynamically significant which can be managed with medical therapy without any downstream testing.[3]

Three large prospective studies, such as the Diagnosis of Ischemia-Causing Stenoses Obtained Via Noninvasive Fractional Flow Reserve (DISCOVER-FLOW), Determination of Fractional Flow Reserve by Anatomic Computed Tomographic Angiography (DeFACTO), and Analysis of Coronary Blood Flow Using CT Angiography: Next Steps (NXT), have evaluated the diagnostic accuracy of CT derived FFR measurements.[48–50] DISCOVER-FLOW reported that the use of FFR_{CT} improves the per-vessel accuracy from 59% (sensitivity, 91% and specificity, 40%) for CCTA alone to 84% (sensitivity, 88% and specificity, 82%) with the addition of CT-FFR. DEFACTO trial reported an improvement in the diagnostic accuracy from 64% (sensitivity, 84% and specificity, 42%) for CCTA alone to 73% (sensitivity, 90% and specificity, 54%) with the addition of CT-FFR. The third NXT trial evaluated 310 patients with both CCTA and CT-FFR and achieved the best precision of the available prospective studies. The results showed an improvement in diagnostic accuracy from 65% (sensitivity, 83% and specificity, 60%) for CCTA alone to 86% (sensitivity, 84% and specificity, 86%) with the addition of CT-FFR.

In summary, CT-FFR has ability to overcome one of the major limitation of CCTA, a low specificity in detecting myocardial ischemia. However, the current use of CT-FFR is limited by challenging workflow, higher cost and limited data on the cost-effectiveness of CCTA alone, and CCTA with functional tests.

Limitations of Cardiac Computed Tomography Imaging

The current restrictions in spatial and temporal resolution make CCTA frequently falls short in assessing the precise degree of stenosis as compared with ICA. The accuracy of CCTA to detect and quantify atherosclerotic plaque is also largely unknown. In comparison to IVUS, the sensitivity of CCTA for identifying plaques have been reported to be approximately 85 to 95% with high interobserver agreement. This high sensitivity is mainly driven by its ability to detect calcified plaque, whereas noncalcified plaque is more difficult to delineate.[51] Similarly, the imaging of coronary stents with CCTA is difficult. The reported positive predictive values of CCTA for in-stent restenosis is low, resulting in a high number of false-positive results. Although, newer technology may offer some improvement, but the evaluation is largely restricted to single stents with a larger diameter (e.g., >3.0 mm).[52,53] Furthermore, CT myocardial perfusion is limited by high radiation dose, artifacts, and large interobserver variability and lack of large-scale multicenter studies demonstrating its clinical value.

Role of Cardiac Magnetic Resonance in Coronary Artery Disease

CMR has emerged as a very useful tool in the evaluation of CAD. It provides valuable and comprehensive information on anatomical and functional assessment of CAD. There is a

growing evidence that CMR is useful in each step of CAD assessment, ranging from establishing the diagnosis, guiding the treatment and risk stratification.[54] Steady-state free precession (SSFP) is the workhorse of the CMR imaging. It is primarily used for volumetry, functional analysis and myocardial mass calculation. T2-weighted turbo spin-echo (SE) sequences are used to detect myocardial edema which is useful in differentiating between acute and chronic myocardial infarction. Single-shot, turbo gradient-echo (GRE) and echo-planar imaging sequences are used for myocardial perfusion imaging. T1-weighted inversion-recovery (IR) sequence with gadolinium administration is used for contrast-enhanced myocardial imaging. T1 and T2 mapping are newer techniques allowing calculation of absolute values of T1 and T2 relaxation times. The benefits of mapping technique include better myocardial characterization with quantitative assessment and decreased intraobserver and interobserver variability. MRI tagging allows visual assessment and quantification of regional myocardial motion. Strain-encoding (SENC) is another magnitude-based technique for assessing regional myocardial motion. Similar to tagging, it is also based on applying parallel planes of saturated pulsed but thorough-plane motion is measured compared with in-plane motion in tagging. SENC has the advantages of higher resolution, faster image acquisition, and generation of color coded strain maps.[55] CMR-feature tracking (CMR-FT) is a newer technique for quantitative evaluation of myocardial function by directly evaluating myocardial fiber deformation. The CMR-FT derived strain parameters can identify subtle myocardial abnormalities before the overt clinical manifestation sets in.[56]

Cardiac Magnetic Resonance for Coronary Imaging

Coronary arteries are difficult to image by CMR for few reasons. These include small vessel caliber, tortuous course, the surrounding signal from myocardium and epicardial fat, continuous motion–related to the cardiac and respiratory cycles, and limited acquisition time in diastole. The development of three-dimensional (3D) acquisition techniques have allowed better image quality. In an international multicenter trial published by Kim et al, the diagnostic accuracy of 3D CMR angiography was compared with ICA. Overall, 84% of the proximal and mid–coronary artery segments were interpretable with a reported sensitivity and specificity of 93 and 42%, respectively, for >50% luminal stenosis.[57] CMR angiography can be used in CABG assessment as grafts are less affected by cardiac and respiratory motion. The artifacts from clips may, however, limit their assessment. CMR is helpful in both anatomic and functional assessment of CABG. The diagnostic accuracy has increased with the introduction of flow velocity mapping techniques but its application in clinical practice is still limited.[58,59]

Coronary stents appear as signal void on CMR angiography making the visualization of stent lumen difficult. However, the flow velocity mapping techniques have shown promising results as with CABG.[60] CMR angiography is an accepted gold standard to assess congenital coronary anomalies. Although, these are rarely seen in general population but are a common cause of sudden cardiac death in athletes.[61] Beside luminography, CMR is also useful for characterization of atherosclerotic plaques. The black blood imaging appears to be promising technique for assessing plaque formation and coronary vessel wall remodeling.[62]

Although, the recent advances such as use of contrast agents, the application of higher field strength and parallel imaging increasing the signal-to-noise ratio leading to better image quality but there are several unresolved issues, like field inhomogeneities, which render the technique prone to several artifacts.[63]

Cardiac Magnetic Resonance in Acute Coronary Syndrome

CMR has a role in the detection of ACS in low-risk patients presenting with chest pain, negative biomarkers, and normal ECG prior to ICA. Study has shown the higher sensitivity and specificity of resting CMR in comparison to ECG, peak troponin-I, and thrombolysis in myocardial infarction (TIMI) risk score $\geq$3, in patients with possible or probable acute coronary syndrome. The sensitivity and specificity of CMR using myocardial perfusion, left ventricular function, and late gadolinium enhancement (LGE) was found to be 84 and 85%, respectively.[64] By adding edema imaging, the diagnostic accuracy further increased up to 93%.[65] In patients with multivessel disease, myocardial edema imaging is helpful in identifying the culprit vessel which is helpful in targeted revascularization.[66]

Cardiac Magnetic Resonance in Non-ST Segment Elevated Acute Coronary Syndrome

CMR is an accurate tool to detect the presence of flow-limiting stenosis in patients with a clinical diagnosis of non-ST segment–elevated (NSTE) ACS. A study conducted by Schroeder et al has reported that comprehensive CMR imaging involving myocardial function assessment, perfusion (rest and adenosine-stress), viability (by LGE), and coronary artery anatomy has a sensitivity of 96% and a specificity of 83% in predicting coronary stenosis. Furthermore, CMR was found to be more sensitive and accurate than TIMI risk score.[67] Approximately 7 to 15% of the patients with ACS and raised troponin levels have no significant CAD on ICA, representing diagnostic dilemma. There are a large number of causes of an elevated troponin in the absence of significant CAD which include infarction with spontaneous recanalization, myocarditis, cardiac contusion, cardiomyopathy, congestive heart failure, and noncardiac causes including sepsis, pulmonary embolism, and renal failure. The presence of myocardial infarction (MI) in the absence of obstructive CAD can be explained by embolism, coronary spasm, and arterial recanalization. CMR provides detailed myocardial tissue characteristics and is helpful in evaluating the ACS with insignificant CAD. The high-contrast and spatial resolution of CMR allow the identification of very small infarcts which may be missed by SPECT. LGE is gold standard

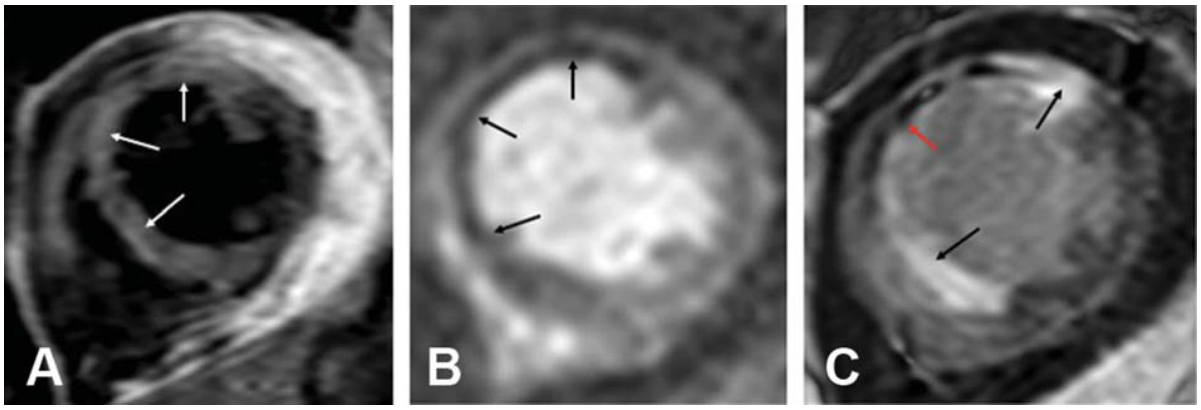

Fig. 14 MR imaging findings in acute MI in a 45-year-old man with sudden onset of chest pain, elevated cardiac enzymes, and ST-segment elevation. (**A**) Short axis T2-weighted short inversion time inversion recovery (STIR) image shows high-signal-intensity edema in the anterior and septal wall (white arrows), consistent with myocardial edema. (**B**) Short-axis dynamic perfusion image shows perfusion defects in anterior and septal wall (black arrows). (**C**) Short-axis delayed-enhancement image shows a full-thickness transmural infarct in the anterior and septal wall (black arrow). Within this area of scar, there is a nonenhancing dark focus (red arrow), consistent with acute microvascular obstruction within an infarct and indicating an area of no-reflow phenomenon.

in detection of scarring associated with various ischemic and nonischemic conditions. Study has shown that CMR can identify the basis for troponin elevation in 65% of patients presenting with ACS type symptoms with insignificant stenosis on coronary angiography.[68]

Cardiac Magnetic Resonance in ST Segment Elevated Acute Coronary Syndrome

The recent availability of multiparametric CMR has provided detailed assessment regarding the pathophysiology of STEMI. The native T1, T2, T2*, and postcontrast T1-mapping provides insights into the evolution of myocardial edema in the first week post-STEMI, prognostic significance of microvascular obstruction, chronic manifestation of intramyocardial hemorrhage, and changes in the remote myocardial interstitial space responsible for adverse left ventricle (LV) remodeling (►**Fig. 14**).[69] CMR also provides information on the cardioprotective efficacy of various treatment methodologies therapies for reducing MI size and prevent adverse LV remodeling in reperfused STEMI patients.[70]

Cardiac Magnetic Resonance in Complications of Acute Coronary Syndrome

CMR is also a helpful tool in identifying the complications of ACS-like ventricular thrombus, ventricular aneurysm, pseudoaneurysm, ventricular septal defects, and papillary muscle infarction with subsequent mitral regurgitation.[71] Right ventricle (RV) infarction occurs in approximately 50% patients with inferior MI. It is associated with a poor prognosis. The established methods are less sensitive in detecting it. CMR can identify the RV infarctions and is a strong predictor of the clinical outcome after reperfusion of acute STEMI.[72]

Cardiac Magnetic Resonance in Chronic Ischemic Heart Disease

Ischemia-induced LV dysfunction is not always an irreversible process. Numerous studies have shown that ischemic LV dysfunction may be reversible (myocardial stunning or hibernation). Myocardial viability is a reflection of ischemia-induced impaired contractility at rest that recovers after revascularization. The assessment of myocardial viability is the cornerstone in guiding the clinical management. Myocardial viability was earlier defined on transthoracic echocardiography (TTE) and PET by means of wall motion abnormalities, LV wall thickness, and reduced metabolism. This concept has been further expanded by CMR which shows better sensitivity, specificity, and accuracy than SPECT in predicting myocardial viability. The commonly used CMR parameters for assessing myocardial viability are infarct transmurality with LGE imaging, coronary reserve with adenosine stress perfusion, and contractile reserve with dobutamine stress.[73]

LGE is based on a pulse sequence that allowed nulling of normal myocardium and demonstrates bright signal in infarcted myocardium when imaged 10 to 20 minutes after gadolinium administration. The fibrotic areas show increased volume of redistribution of gadolinium, as well as delayed washout, and hence appear bright. The evaluation of the transmural extent of LGE has been shown to be a predictor of LV function recovery with revascularization. In a study done by Kim et al, the absence of LGE corresponded to 78% chances of recovery at 3 months, compared with 59% with 1 to 25% LGE transmurality, falling to 2% with >75% LGE transmurality.[74] Another study reported 82% chances of recovery with no preexisting LGE, 64% with 1 to 25% LGE transmurality, and 37% with 26 to 50% LGE transmurality.[75]

Dobutamine stress CMR is aimed at detecting the contractile reserve of the myocardium. Dobutamine is a synthetic β_1 adrenergic catecholamine having positive inotropic effect. The protocol for dobutamine stress CMR follows the echocardiography protocol: dobutamine is administered at increasing doses until target heart rate is achieved. The infusion of dobutamine leads to increased myocardial oxygen consumption which cannot be compensated by significantly occluded coronary arteries, leading to ischemia and

decreased myocardial contractility. If there is a flow limiting stenotic lesion in coronary, the myocardium will display new regional wall motion abnormality on cine images which is a surrogate for ischemia. Conversely, any improvement in the regional wall motion abnormality after low dose dobutamine administration represents a marker for myocardial viability. The image analysis is done by both visual and quantitative methods and the findings are documented on the 17-segment model. The hibernating and stunned myocardium (dysfunctional but viable) show improvement of systolic contraction and wall thickening at low dose dobutamine infusion (5–10 µg/kg/min). High-dose protocols (up to 40 µg/kg/min) are used to demonstrate the biphasic response; improvement in the contractile function at low dose and worsening of the contractile function at high dose caused by stress-induced ischaemia.[76] The sensitivity and specificity of dobutamine CMR in predicting functional recovery has been reported in the range from 50 to 82 and 81 to 90%, respectively. The adoption of quantitative assessment methods further increase the sensitivity and specificity as high as 89 and 93%, respectively.[77]

Adenosine stress perfusion CMR is aimed at detecting the coronary flow reserve. The myocardial blood flow may remain normal for up to approximately 85% stenosis of the epicardial coronary artery at rest and get reduced during maximal hyperemia unveiling underlying autoregulatory decompensation at the level of the microvascular bed. A variety of pulse sequences are currently available for perfusion imaging including gradient-echo (GRE), hybrid GRE–echo-planar imaging (EPI), and SSFP sequences. The selection of correct sequence is critical in determining spatial resolution, image contrast, coverage, potential for quantification, and presence of artifacts.[78] Adenosine is most commonly used vasodilator agent. The protocol involves both stress and rest examinations. Adenosine is infused intravenously at the rate of 140 µg/kg/min for at least 3 minutes to achieve peak vasodilatation. Continuous monitoring of ECG, blood pressure, and patients symptoms are done simultaneously. Images are acquired at selected long- and short-axis planes on every heartbeat (for 50 beats) while patients are holding their breath. The infusion is then stopped and gadolinium is administered. Subsequently, early postgadolinium imaging is performed to demonstrate microvascular obstruction which is seen as areas of low signal in subendocardial distribution. The rest perfusion is done approximately 20 minutes after the completion of the adenosine infusion. The combined assessment of rest and stress first-pass perfusion images are used to differentiate induced perfusion defects and ischemia.[79] Multiple trials have compared the CMR perfusion with PET and SPECT. In a meta-analysis of 12 studies using FFR as a reference standard, CMR perfusion has shown a sensitivity of 89.1% and specificity of 84.9% on a patient basis, as well as a sensitivity of 87.7% and specificity of 88.6% on a coronary territory basis.[80] A study done by Nandalur et al has showed that perfusion CMR has a sensitivity and specificity of 91 and 81%, respectively, in a per-patient analysis for the identification of the ischemic segments.[81] A large prospective randomized trial has shown superior sensitivity and negative predictive value of perfusion CMR compared with SPECT.[82]

Limitations of Cardiac Magnetic Resonance

Though CMR is increasingly being used in clinical practice, its availability is still limited in many centers. There are many contraindications to CMR including claustrophobia, severe dyspnea, arrhythmia, and clinically unstable conditions. Patients with non-MR conditional devices (neurostimulator, intracranial clips, and metallic objects) must not be offered a CMR. Recent advancements in technology allow the imaging of patients with MR-conditional cardiac devices (pace-maker and implantable cardioverter defibrillator [ICD]), though under strict medical monitoring. Furthermore, the gadolinium-based contrast agents, although safer than iodine contrast, should be avoided in severe renal dysfunction due to the risk of potentially fatal nephrogenic systemic fibrosis.

Conclusion

Cardiac CT and CMR imaging have emerged as the most promising complementary imaging techniques in the primary diagnosis of CAD. The combined applications of cardiac CT and CMR can exclude the CAD with a high probability. To derive the most benefit from these technique, patient selection remains a key issue. The appropriate use largely depend on patient characteristics and the clinical question. New technologies and new applications are constantly being explored and are widening the scope of both modalities for the complete analysis of cardiac morphology, function, perfusion, and viability. One should consider cardiac CT and CMR as a complementary tools for the noninvasive evaluation of CAD, with inherent limitations but also unique advantages.

Conflict of Interest
None declared.

References

1 Virani SS, Alonso A, Benjamin EJ, et al; American Heart Association Council on Epidemiology and Prevention Statistics Committee and Stroke Statistics Subcommittee. Heart disease and stroke statistics-2020 update: a report from the American Heart Association. Circulation 2020;141(09):e139–e596
2 Bastarrika G, Lee YS, Huda W, Ruzsics B, Costello P, Schoepf UJ. CT of coronary artery disease. Radiology 2009;253(02): 317–338
3 Nørgaard BL, Fairbairn TA, Safian RD, et al. Coronary CT angiography-derived fractional flow reserve testing in patients with stable coronary artery disease: recommendations on interpretation and reporting. Radiol Cardiothorac Imaging 2019;1(05):e190050
4 Baritussio A, Scatteia A, Bucciarelli-Ducci C. Role of cardiovascular magnetic resonance in acute and chronic ischemic heart disease. Int J Cardiovasc Imaging 2018;34(01):67–80
5 Yerramasu A, Venuraju S, Lahiri A. Evolving role of cardiac CT in the diagnosis of coronary artery disease. Postgrad Med J 2011;87 (1025):180–188
6 Sandfort V, Bluemke DA. CT calcium scoring. History, current status and outlook. Diagn Interv Imaging 2017;98(01):3–10

7 Agatston AS, Janowitz WR, Hildner FJ, Zusmer NR, Viamonte M Jr, Detrano R. Quantification of coronary artery calcium using ultrafast computed tomography. J Am Coll Cardiol 1990;15(04): 827–832

8 Hecht HS, Blaha MJ, Kazerooni EA, et al. CAC-DRS: coronary artery calcium data and reporting system. An expert consensus document of the Society of Cardiovascular Computed Tomography (SCCT). J Cardiovasc Comput Tomogr 2018;12(03):185–191

9 Dzaye O, Dudum R, Mirbolouk M, et al. Validation of the coronary artery calcium data and reporting system (CAC-DRS): dual importance of CAC score and CAC distribution from the Coronary Artery Calcium (CAC) consortium. J Cardiovasc Comput Tomogr 2020;14(01):12–17

10 Osawa K, Bessho A, Fuke S, et al. Coronary artery calcification scoring system based on the coronary artery calcium data and reporting system (CAC-DRS) predicts major adverse cardiovascular events or all-cause death in patients with potentially curable lung cancer without a history of cardiovascular disease. Heart Vessels 2020;35(11):1483–1493

11 von Ballmoos MW, Haring B, Juillerat P, Alkadhi H. Meta-analysis: diagnostic performance of low-radiation-dose coronary computed tomography angiography. Ann Intern Med 2011;154(06): 413–420

12 Schuetz GM, Zacharopoulou NM, Schlattmann P, Dewey M. Meta-analysis: noninvasive coronary angiography using computed tomography versus magnetic resonance imaging. Ann Intern Med 2010;152(03):167–177

13 Pontone G, Andreini D, Bartorelli AL, et al. Radiation dose and diagnostic accuracy of multidetector computed tomography for the detection of significant coronary artery stenoses: a meta-analysis. Int J Cardiol 2012;160(03):155–164

14 Raff GL, Chinnaiyan KM, Cury RC, et al; Society of Cardiovascular Computed Tomography Guidelines Committee. SCCT guidelines on the use of coronary computed tomographic angiography for patients presenting with acute chest pain to the emergency department: a report of the Society of Cardiovascular Computed Tomography Guidelines Committee. J Cardiovasc Comput Tomogr 2014;8(04):254–271

15 Abbara S, Blanke P, Maroules CD, et al. SCCT guidelines for the performance and acquisition of coronary computed tomographic angiography: a report of the Society of Cardiovascular Computed Tomography Guidelines Committee: Endorsed by the North American Society for Cardiovascular Imaging (NASCI). J Cardiovasc Comput Tomogr 2016;10(06):435–449

16 Raff GL, Abidov A, Achenbach S, et al; Society of Cardiovascular Computed Tomography. SCCT guidelines for the interpretation and reporting of coronary computed tomographic angiography. J Cardiovasc Comput Tomogr 2009;3(02):122–136

17 Hendel RC, Patel MR, Kramer CM, et al; American College of Cardiology Foundation Quality Strategic Directions Committee Appropriateness Criteria Working Group American College of Radiology Society of Cardiovascular Computed Tomography Society for Cardiovascular Magnetic Resonance American Society of Nuclear Cardiology North American Society for Cardiac Imaging Society for Cardiovascular Angiography and Interventions Society of Interventional Radiology. ACCF/ACR/SCCT/SCMR/ASNC/NASCI/SCAI/SIR 2006 appropriateness criteria for cardiac computed tomography and cardiac magnetic resonance imaging: a report of the American College of Cardiology Foundation Quality Strategic Directions Committee Appropriateness Criteria Working Group, American College of Radiology, Society of Cardiovascular Computed Tomography, Society for Cardiovascular Magnetic Resonance, American Society of Nuclear Cardiology, North American Society for Cardiac Imaging, Society for Cardiovascular Angiography and Interventions, and Society of Interventional Radiology. J Am Coll Cardiol 2006;48(07):1475–1497

18 Budoff MJ, Dowe D, Jollis JG, et al. Diagnostic performance of 64-multidetector row coronary computed tomographic angiography for evaluation of coronary artery stenosis in individuals without known coronary artery disease: results from the prospective multicenter ACCURACY (Assessment by Coronary Computed Tomographic Angiography of Individuals Undergoing Invasive Coronary Angiography) trial. J Am Coll Cardiol 2008;52(21): 1724–1732

19 Raff GL, Gallagher MJ, O'Neill WW, Goldstein JA. Diagnostic accuracy of noninvasive coronary angiography using 64-slice spiral computed tomography. J Am Coll Cardiol 2005;46(03): 552–557

20 Miller JM, Rochitte CE, Dewey M, et al. Diagnostic performance of coronary angiography by 64-row CT. N Engl J Med 2008;359(22): 2324–2336

21 Achenbach S, Moselewski F, Ropers D, et al. Detection of calcified and noncalcified coronary atherosclerotic plaque by contrast-enhanced, submillimeter multidetector spiral computed tomography: a segment-based comparison with intravascular ultrasound. Circulation 2004;109(01):14–17

22 Cury RC, Abbara S, Achenbach S, et al; Endorsed by the American College of Cardiology. CAD-RADS(TM) coronary artery disease - reporting and data system. An expert consensus document of the Society of Cardiovascular Computed Tomography (SCCT), the American College of Radiology (ACR) and the North American Society for Cardiovascular Imaging (NASCI). J Cardiovasc Comput Tomogr 2016;10(04):269–281

23 Gilard M, Cornily JC, Pennec PY, et al. Assessment of coronary artery stents by 16 slice computed tomography. Heart 2006;92 (01):58–61

24 Li Y, Yu M, Li W, Lu Z, Wei M, Zhang J. Third generation dual-source CT enables accurate diagnosis of coronary restenosis in all size stents with low radiation dose and preserved image quality. Eur Radiol 2018;28(06):2647–2654

25 Mahnken AH. CT imaging of coronary stents: past, present, and future. ISRN Cardiol 2012;2012:139823

26 Barbero U, Iannaccone M, d'Ascenzo F, et al. 64 slice-coronary computed tomography sensitivity and specificity in the evaluation of coronary artery bypass graft stenosis: a meta-analysis. Int J Cardiol 2016;216:52–57

27 Oraby AS, Alarabawy RA, Abd Alla TM, et al. High risk plaque criteria by multislice coronary CT angiography in patients with stable vs. unstable coronary artery disease: analytic cross-sectional study. Egypt J Radiol Nucl Med 2020;51:21

28 Motoyama S, Sarai M, Harigaya H, et al. Computed tomographic angiography characteristics of atherosclerotic plaques subsequently resulting in acute coronary syndrome. J Am Coll Cardiol 2009;54(01):49–57

29 Otsuka K, Fukuda S, Tanaka A, et al. Napkin-ring sign on coronary CT angiography for the prediction of acute coronary syndrome. JACC Cardiovasc Imaging 2013;6(04):448–457

30 Puchner SB, Liu T, Mayrhofer T, et al. High-risk plaque detected on coronary CT angiography predicts acute coronary syndromes independent of significant stenosis in acute chest pain: results from the ROMICAT-II trial. J Am Coll Cardiol 2014;64(07): 684–692

31 De Cecco CN, Varga-Szemes A, Meinel FG, Renker M, Schoepf UJ. Beyond stenosis detection: computed tomography approaches for determining the functional relevance of coronary artery disease. Radiol Clin North Am 2015;53(02):317–334

32 Varga-Szemes A, Meinel FG, De Cecco CN, Fuller SR, Bayer RR II, Schoepf UJ. CT myocardial perfusion imaging. AJR Am J Roentgenol 2015;204(03):487–497

33 Cademartiri F, Seitun S, Clemente A, et al. Myocardial blood flow quantification for evaluation of coronary artery disease by computed tomography. Cardiovasc Diagn Ther 2017;7(02): 129–150

34 Mehra VC, Valdiviezo C, Arbab-Zadeh A, et al. A stepwise approach to the visual interpretation of CT-based myocardial perfusion. J Cardiovasc Comput Tomogr 2011;5(06):357–369

35 Nasis A, Ko BS, Leung MC, et al. Diagnostic accuracy of combined coronary angiography and adenosine stress myocardial perfusion imaging using 320-detector computed tomography: pilot study. Eur Radiol 2013;23(07):1812–1821

36 George RT, Mehra VC, Chen MY, et al. Myocardial CT perfusion imaging and SPECT for the diagnosis of coronary artery disease: a head-to-head comparison from the CORE320 multicenter diagnostic performance study. Radiology 2015;274(02):626–626

37 Schwarz F, Ruzsics B, Schoepf UJ, et al. Dual-energy CT of the heart–principles and protocols. Eur J Radiol 2008;68(03):423–433

38 Johnson TR, Krauss B, Sedlmair M, et al. Material differentiation by dual energy CT: initial experience. Eur Radiol 2007;17(06): 1510–1517

39 De Cecco CN, Harris BS, Schoepf UJ, et al. Incremental value of pharmacological stress cardiac dual-energy CT over coronary CT angiography alone for the assessment of coronary artery disease in a high-risk population. AJR Am J Roentgenol 2014;203(01): W70-7

40 Rubinshtein R, Miller TD, Williamson EE, et al. Detection of myocardial infarction by dual-source coronary computed tomography angiography using quantitated myocardial scintigraphy as the reference standard. Heart 2009;95(17):1419–1422

41 Bauer RW, Kerl JM, Fischer N, et al. Dual-energy CT for the assessment of chronic myocardial infarction in patients with chronic coronary artery disease: comparison with 3-T MRI. AJR Am J Roentgenol 2010;195(03):639–646

42 Caruso D, Eid M, Schoepf UJ, et al. Dynamic CT myocardial perfusion imaging. Eur J Radiol 2016;85(10):1893–1899

43 Bastarrika G, Ramos-Duran L, Rosenblum MA, Kang DK, Rowe GW, Schoepf UJ. Adenosine-stress dynamic myocardial CT perfusion imaging: initial clinical experience. Invest Radiol 2010;45(06): 306–313

44 Ho KT, Chua KC, Klotz E, Panknin C. Stress and rest dynamic myocardial perfusion imaging by evaluation of complete time-attenuation curves with dual-source CT. JACC Cardiovasc Imaging 2010;3(08):811–820

45 Strisciuglio T, Barbato E. The fractional flow reserve gray zone has never been so narrow. J Thorac Dis 2016;8(11):E1537–E1539

46 Tonino PA, Fearon WF, De Bruyne B, et al. Angiographic versus functional severity of coronary artery stenoses in the FAME study fractional flow reserve versus angiography in multivessel evaluation. J Am Coll Cardiol 2010;55(25):2816–2821

47 Taylor CA, Fonte TA, Min JK. Computational fluid dynamics applied to cardiac computed tomography for noninvasive quantification of fractional flow reserve: scientific basis. J Am Coll Cardiol 2013;61(22):2233–2241

48 Koo BK, Erglis A, Doh JH, et al. Diagnosis of ischemia-causing coronary stenoses by noninvasive fractional flow reserve computed from coronary computed tomographic angiograms. Results from the prospective multicenter DISCOVER-FLOW (Diagnosis of Ischemia-Causing Stenoses Obtained Via Noninvasive Fractional Flow Reserve) study. J Am Coll Cardiol 2011;58(19):1989–1997

49 Min JK, Leipsic J, Pencina MJ, et al. Diagnostic accuracy of fractional flow reserve from anatomic CT angiography. JAMA 2012;308(12):1237–1245

50 Nørgaard BL, Leipsic J, Gaur S, et al; NXT Trial Study Group. Diagnostic performance of noninvasive fractional flow reserve derived from coronary computed tomography angiography in suspected coronary artery disease: the NXT trial (Analysis of Coronary Blood Flow Using CT Angiography: Next Steps). J Am Coll Cardiol 2014;63(12):1145–1155

51 Leber AW, Becker A, Knez A, et al. Accuracy of 64-slice computed tomography to classify and quantify plaque volumes in the proximal coronary system: a comparative study using intravascular ultrasound. J Am Coll Cardiol 2006;47(03):672–677

52 Hendel RC, Patel MR, Kramer CM, et al; American College of Cardiology Foundation Quality Strategic Directions Committee Appropriateness Criteria Working Group American College of Radiology Society of Cardiovascular Computed Tomography Society for Cardiovascular Magnetic Resonance American Society of Nuclear Cardiology North American Society for Cardiac Imaging Society for Cardiovascular Angiography and Interventions Society of Interventional Radiology. ACCF/ACR/SCCT/SCMR/ASNC/NASCI/SCAI/SIR 2006 appropriateness criteria for cardiac computed tomography and cardiac magnetic resonance imaging: a report of the American College of Cardiology Foundation Quality Strategic Directions Committee Appropriateness Criteria Working Group, American College of Radiology, Society of Cardiovascular Computed Tomography, Society for Cardiovascular Magnetic Resonance, American Society of Nuclear Cardiology, North American Society for Cardiac Imaging, Society for Cardiovascular Angiography and Interventions, and Society of Interventional Radiology. J Am Coll Cardiol 2006;48(07):1475–1497

53 Schroeder S, Achenbach S, Bengel F, et al; Working Group Nuclear Cardiology and Cardiac CT European Society of Cardiology European Council of Nuclear Cardiology. Cardiac computed tomography: indications, applications, limitations, and training requirements: report of a Writing Group deployed by the Working Group Nuclear Cardiology and Cardiac CT of the European Society of Cardiology and the European Council of Nuclear Cardiology. Eur Heart J 2008;29(04):531–556

54 Florian A, Jurcut R, Ginghina C, Bogaert J. Cardiac magnetic resonance imaging in ischemic heart disease: a clinical review. J Med Life 2011;4(04):330–345

55 Lee E, Ibrahim EH, Parwani P, Bhave N, Stojanovska J. Practical guide to evaluating myocardial disease by cardiac MRI. AJR Am J Roentgenol 2020;214(03):546–556

56 Muser D, Castro SA, Santangeli P, Nucifora G. Clinical applications of feature-tracking cardiac magnetic resonance imaging. World J Cardiol 2018;10(11):210–221

57 Kim WY, Danias PG, Stuber M, et al. Coronary magnetic resonance angiography for the detection of coronary stenoses. N Engl J Med 2001;345(26):1863–1869

58 Langerak SE, Vliegen HW, Jukema JW, et al. Value of magnetic resonance imaging for the noninvasive detection of stenosis in coronary artery bypass grafts and recipient coronary arteries. Circulation 2003;107(11):1502–1508

59 Salm LP, Bax JJ, Vliegen HW, et al. Functional significance of stenoses in coronary artery bypass grafts. Evaluation by single-photon emission computed tomography perfusion imaging, cardiovascular magnetic resonance, and angiography. J Am Coll Cardiol 2004;44(09):1877–1882

60 Nagel E, Thouet T, Klein C, et al. Noninvasive determination of coronary blood flow velocity with cardiovascular magnetic resonance in patients after stent deployment. Circulation 2003;107 (13):1738–1743

61 Post JC, van Rossum AC, Bronzwaer JG, et al. Magnetic resonance angiography of anomalous coronary arteries. A new gold standard for delineating the proximal course? Circulation 1995;92(11): 3163–3171

62 Fayad ZA, Fuster V, Fallon JT, et al. Noninvasive in vivo human coronary artery lumen and wall imaging using black-blood magnetic resonance imaging. Circulation 2000;102(05):506–510

63 Sakuma H, Ichikawa Y, Suzawa N, et al. Assessment of coronary arteries with total study time of less than 30 minutes by using whole-heart coronary MR angiography. Radiology 2005;237(01): 316–321

64 Kwong RY, Schussheim AE, Rekhraj S, et al. Detecting acute coronary syndrome in the emergency department with cardiac magnetic resonance imaging. Circulation 2003;107(04):531–537

65 Cury RC, Shash K, Nagurney JT, et al. Cardiac magnetic resonance with T2-weighted imaging improves detection of patients with acute coronary syndrome in the emergency department. Circulation 2008;118(08):837–844

66 Raman SV, Simonetti OP, Winner MW III, et al. Cardiac magnetic resonance with edema imaging identifies myocardium at risk and

predicts worse outcome in patients with non-ST-segment elevation acute coronary syndrome. J Am Coll Cardiol 2010;55(22):2480–2488
67 Plein S, Greenwood JP, Ridgway JP, Cranny G, Ball SG, Sivananthan MU. Assessment of non-ST-segment elevation acute coronary syndromes with cardiac magnetic resonance imaging. J Am Coll Cardiol 2004;44(11):2173–2181
68 Assomull RG, Lyne JC, Keenan N, et al. The role of cardiovascular magnetic resonance in patients presenting with chest pain, raised troponin, and unobstructed coronary arteries. Eur Heart J 2007; 28(10):1242–1249
69 Fernández-Jiménez R, Barreiro-Pérez M, Martin-García A, et al. Dynamic Edematous Response of the Human Heart to Myocardial Infarction: Implications for Assessing Myocardial Area at Risk and Salvage. Circulation 2017;136(14):1288–1300
70 Bulluck H, Dharmakumar R, Arai AE, Berry C, Hausenloy DJ. Cardiovascular Magnetic Resonance in Acute ST-Segment-Elevation Myocardial Infarction: Recent Advances, Controversies, and Future Directions. Circulation 2018;137(18):1949–1964
71 Stephens NR, Restrepo CS, Saboo SS, Baxi AJ. Overview of complications of acute and chronic myocardial infarctions: revisiting pathogenesis and cross-sectional imaging. Postgrad Med J 2019; 95(1126):439–450
72 Kumar A, Abdel-Aty H, Kriedemann I, et al. Contrast-enhanced cardiovascular magnetic resonance imaging of right ventricular infarction. J Am Coll Cardiol 2006;48(10):1969–1976
73 Catalano O, Moro G, Mori A, et al. Cardiac magnetic resonance in stable coronary artery disease: added prognostic value to conventional risk profiling. BioMed Res Int 2018;2018:2806148
74 Kim RJ, Wu E, Rafael A, et al. The use of contrast-enhanced magnetic resonance imaging to identify reversible myocardial dysfunction. N Engl J Med 2000;343(20):1445–1453
75 Selvanayagam J, Kardos A, Francis J. Value of delayed-enhancement cardiovascular magnetic resonance imaging in predicting myocardial viability after surgical revascularization. ACC Curr J Rev 2005;14(01):28
76 Strach K, Meyer C, Schild H, Sommer T. Cardiac stress MR imaging with dobutamine. Eur Radiol 2006;16(12):2728–2738
77 Schmidt A, Wu KC. MRI assessment of myocardial viability. Semin Ultrasound CT MR 2006;27(01):11–19
78 Coelho-Filho OR, Rickers C, Kwong RY, Jerosch-Herold M. MR myocardial perfusion imaging. Radiology 2013;266(03):701–715
79 Raj V, Agrawal SK. Ischaemic heart disease assessment by cardiovascular magnetic resonance imaging. Postgrad Med J 2010;86 (1019):532–540
80 Desai RR, Jha S. Diagnostic performance of cardiac stress perfusion MRI in the detection of coronary artery disease using fractional flow reserve as the reference standard: a meta-analysis. AJR Am J Roentgenol 2013;201(02):W245-52
81 Nandalur KR, Dwamena BA, Choudhri AF, Nandalur MR, Carlos RC. Diagnostic performance of stress cardiac magnetic resonance imaging in the detection of coronary artery disease: a meta-analysis. J Am Coll Cardiol 2007;50(14):1343–1353
82 Greenwood JP, Maredia N, Younger JF, et al. Cardiovascular magnetic resonance and single-photon emission computed tomography for diagnosis of coronary heart disease (CE-MARC): a prospective trial. Lancet 2012;379(9814):453–460

